SUPPLEMENTAL EXPERIMENTAL PROCEDURES

Deletion of NELF-B in Adult Mice

All of the animal experiment procedures were approved by the Institutional Animal Care and Use Committee (IACUC). For deletion of the floxed NELF-B allele via the CAG-Cre-ER^{TM} transgenic system, mice of 8 to 10 weeks old were treated with tamoxifen (TAM; Sigma, Cat. #T5648). TAM was solubilized at 10 mg/ml in sunflower oil and delivered into mice by intraperitoneal injection for five consecutive days at 100 mg/kg/day. For deletion of the floxed NELF-B allele using the α-MHC-MerCreMer transgenic system, mice were treated with TAM for four consecutive days at a dose of 40 mg/kg/day. Genotyping primers used to confirm the gene deletion were described previously (Amleh et al., 2009).

Histology and Picrosirius Red Staining

The left ventricle was divided into 3 sections with similar thickness. The mid-papillary section was fixed in 10% zinc-formalin overnight at room temperature and dehydrated with ethanol. The tissues were then embedded in paraffin and sectioned at 5 μm. Hematoxylin and eosin (H&E) staining was used for inflammatory cell assessment and to measure the cross-sectional areas of cardiomyocytes as previously described (Lindsey et al., 2003). For the picrosirius red staining to evaluate the extent of collagen deposition, the sections were incubated with 0.1% Sirius Red (Electron Microscopy Sciences, Cat. #26357-02) in saturated picric acid for 90 min and washed in 0.01 N

hydrochloric acid solution for 2 min. Five random sections were imaged and analyzed with Image-Pro Plus (Bethesda, MD, USA) as described previously (Lin et al., 2008).

Neutrophil Immunohistochemistry

LV sections embedded in paraffin were de-paraffinized with xylene and rehydrated with a graded decrease of alcohol to water. For antigen retrieval, slides were submerged in Dako Target Retrieval Solution (Dako, Carpinteria, CA) and heated to 96°C for 10 min. Slides were cooled to room temperature for 20 min and washed twice in water for 5 min. Endogenous peroxidases were blocked by incubation in 3% hydrogen peroxide in water for 20 min. Slides were incubated with the primary antibody, Ly-6B.2 Alloantigen Rat Anti-mouse primary antibody (ABD Serotech, Raleigh, NC) in 1:100 dilution, overnight at 4°C. Slides were washed three times with PBS, then incubated with biotinylated anti-rat (Vector Laboratories) secondary antibody at a 1:100 dilution for 30 min at room temperature. The slides were washed three times with PBS, then a Vectastain Universal ABC Kit (Vector Laboratories; Burlingame, CA) followed by a Histomark Black Kit (KPL, Gaithersburg, Maryland) was used to visualize the samples.

For neutrophil numeration, 5-7 images from each heart sample were captured at 4x magnification. Image correction and quantification were accomplished with ImageJ. For each image, uneven image illumination was corrected using the ImageJ "Shading Correction" plugin (http://rsbweb.nih.gov/ij/plugins/shading-corrector.html). White background was selected and subtracted from each image using the Default auto-threshold setting. The pixel area of heart tissue was converted to mm^2. The number of

neutrophils in each image was recorded and the total number from all of the images was averaged and divided by the area of the image to determine the number of neutrophils per mm^2 for each heart.

Echocardiography

Mice were anesthetized with 1-2% isoflurane in an oxygen mix. Electrocardiogram and heart rate were monitored throughout the imaging procedure. Measurements were taken from the parasternal long axis M-mode views. For each parameter, three cardiac cycles were measured and averaged. Following the acquisition of baseline images, stress echocardiography was acquired at 30 min after intraperitoneal injection of dobutamine (3 μg/g body weight)(Chiao et al., 2012). The comparison was analyzed among 4 groups (control and KO mice under baseline and dobutamine-stressed conditions at the same time point).

Expression Profiling Analysis in WT versus NELF-B KO Hearts

The left ventricle (LV) of three pairs of control (NELF-$B^{f/f}$) and NELF-B KO (NELF-$B^{f/f}$;CreER) hearts were harvested from 20-week old female mice. Total RNA was then extracted from left ventricles with the miRNeasy mini kit (Qiagen, Cat. #217004) according to the manufacturer's instruction. RNAs were labeled using the Illumina® TotalPrepTM RNA amplification kit (Ambion, Cat. #AMIL1791) and subsequently hybridized to Illumina mouse whole genome gene expression BeadChips (MouseRef-8 version 2.0, Illumina) following published procedures (Kuhn et al., 2004). BeadChips were scanned on a BeadArrayTM Reader (Illumina) using BeadScan software

(version 3.2, Illumina). For further analysis, the scanned data were uploaded into GenomeStudio® software (version 1.1, Illumina) via the gene expression module (Direct Hyb). The DAVID online program was used for gene ontology analysis. The microarray data are available at NIH Gene Expression Omnibus site (GSE54372).

Quantitative RT-PCR

Left ventricle (LV) of heart tissue was extracted with Trizol reagent (Invitrogen, Cat. #15596018). Samples were sonicated using a probe sonicator (Branson, Digital Sonifier 450) at 25% output for 10 seconds. RNA was treated with DNase I (Roche, Cat. #04716728001). cDNA was synthesized with 1 μg of total RNA using the ImPromII Reverse Transcription System (Promega, Cat. #A3800) and random primers. Primers for analysis of gene expression are listed in Supplemental Table S4. Procedures for quantitative real-time PCR have been described previously (Sun et al., 2011), using the 7900HT Real-Time PCR System (Applied Biosystems). The levels of 18sRNA were measured as the internal control.

Chromatin Immunoprecipitation (ChIP)

Control (NELF-B$^{f/f}$) and NELF-B KO (NELF-B$^{f/f}$;CreER) hearts were harvested from 32-week old mice. After rinsing with phosphate buffered saline or PBS, tissue was immediately cut into small pieces and crosslinked in 1% formaldehyde in PBS solution for 15 min at room temperature. After fixation, glycine was added into the formaldehyde solution to a final concentration of 125 mM for 5 min, followed by rinsing with ice-cold PBS and suspension in PBS containing a cocktail of protease inhibitors including

pepstatin (Sigma, Cat. #P5318), aprotinin (Sigma, Cat. #A4529) and leupeptin (Sigma, Cat. #L5793) with the final concentration of 1μg/ml for each. Tissue was homogenized with a 1-ml tissue grinder (Wheaton, Cat. #357538), pelleted, and weighted. 500 μl Lysis Buffer (50 mM Tris at pH 8.0, 10 mM ethylenediaminetetraacetic acid or EDTA at pH 8.0, 1% sodium dodecyl sulfate or SDS, and the cocktail of protease inhibitors as shown above, 1 mM phenylmethanesulfonylfluoride or PMSF) was added to 100 mg tissue. Sonication was performed in 1.5 ml tubes with a probe sonicator (Branson, Digital Sonifier 450) at 25% output for 4 cycles, 10 seconds per cycle. Supernatant was collected after centrifuged at 14,000 rpm for 10 min at 4 °C. Approximately 100 μl supernatant was used per ChIP reaction, followed by 1:10 dilution in ChIP buffer (150 mM NaCl, 25 mM Tris at pH 8.0, 5 mM EDTA at pH 8, 1% Triton X-100, 0.1% SDS, 0.5% sodium doxycholate, the cocktail of protease inhibitors as shown above, 1 mM PMSF). ChIP reactions were carried out as previously described (Sun et al., 2011). Primers for ChIP were provided in Supplemental Table S4. The following commercially available antibodies were used in ChIP: anti-Pol II (Abcam; Cat. #Ab5408), anti-Ser5Pol II (Abcam; Cat. #Ab5131), anti-TFIIB (Santa Cruz; Cat. #sc-225), anti-TFIID (TBP) (Santa Cruz; Cat. #sc-204), anti-RXRα (Santa Cruz; Cat. #sc–553), and anti-histone H3 (Cell Signaling; Cat. #9715). Anti-NELF antibodies used in ChIP assay have been previously described (Sun et al., 2007).

Metabolomic profiling using HPLC-Electrospray Ionization-Tandem Mass Spectrometry (HPLC-ESI-MS/MS)

The left ventricle (LV) of heart tissue was rinsed with PBS, snap-frozen, and pulverized in a mortar and pestle under liquid nitrogen. Metabolites were extracted using ice-cold chloroform/methanol (2:1) and maintained on ice for 30 min as described (Gao et al., 2012). After centrifugation at 13,800 x g for 10 min, the methanol layers were removed and used for polar metabolite analysis. The chloroform layers were dried and reconstituted in isopropanol. HPLC-ESI/MS analyses were conducted on a Thermo Fisher Q Exactive mass spectrometer with on-line separation using either a Thermo Fisher/Dionex RSLC nano HPLC (for lipids) or an Ultimate 3000 HPLC (for polar metabolites). HPLC conditions for lipid analysis were: column, Atlantis dC18 (3 μm, 300 μm x 150 mm; Waters); mobile phase A, acetonitrile/water (40:60) containing 10 mM ammonium acetate; mobile phase B, acetonitrile/isopropanol (10:90) containing 10 mM ammonium acetate; flow rate, 6 μl/min; gradient, 10% B to 60% B over 5 min, 60% B to 99% B over 35 min and held at 99% B for 10 min. HPLC conditions for polar metabolite analysis were: column, Luna NH2 (3 μm, 1mm x 150 mm; Phenomenex); mobile phase A, 5% acetonitrile in water containing 20 mM ammonium acetate and 20 mM ammonium hydroxide, pH 9.45; mobile phase B, acetonitrile; flow rate, 50 μL/min; gradient, 85% B to 1% B over 10 min and held at 1% B for 10 min. For both analyses, data-dependent MS/MS scans were acquired using one full MS scan (*m/z* 200 – 2000 for lipid analysis and *m/z* 85 – 1000 for polar metabolite analysis) followed by 6 MS/MS scans in the HCD collision cell (35% relative collision energy).

Progenesis CoMet (Nonlinear Dynamics) was used to process the raw Q Exactive data files to detect the metabolites that exhibit significant differences in intensity between

the wild type and mutant samples. After peak alignment by the software, integrated peak areas were used to determine the relative abundance of each metabolite. Metabolites that were significantly different ($p<0.05$; Student's *t*-test) were identified based on molecular mass by searching the METLIN Metabolite Search (http://metlin.scripps.edu/metabo_search_alt2.php) and Lipid Maps (http://www.lipidmaps.org/data/databases.html) databases (5-ppm mass tolerance) and manual interpretation of the tandem-MS fragmentation patterns. Comparison with the retention times of commercially available standards was also performed when possible.

Immunoblotting

Immunoblotting was performed as previously described (Aiyar et al., 2004). The commercial antibodies used were: anti-Cpt1b (LifeSpan BioSciences; Cat. #LS-C111098); anti-Idh3g (Santa Cruz; Cat. #sc-55679); anti-RXRα (Santa Cruz; Cat. #sc-553); anti-PPARα (Santa Cruz; Cat. #sc-9000); anti-Cdk9 (Santa Cruz; Cat. #sc-sc-8338) and anti-Cyclin T1 (Santa Cruz; Cat. #sc-10750). The anti-PGC1α antibody was generously provided by Dr. Daniel Kelly.

Gene Set Enrichment Analysis

To determine whether genes down- or up-regulated in NELF-B KO mice were similarly regulated in PPARα KO mice, NELF-B KO dataset was compared with the previously reported PPARα KO gene expression dataset. Genes down-regulated in NELF-B KO mice were first identified, and their fold of changes was obtained from the

dataset for the PPARα KO mice. An enrichment score (ES) was then calculated using following formula:

$ES = \Sigma X_i/n$ n: number of genes

$X_i = \log_2(FC_i)$ FC_i: fold of change of gene i in PPARα KO mice

If the set of genes were down-regulated in PPARα KO mice as well, the ES value should be negative. This ES value was termed ES_0. To obtain statistical significance of ES_0, we randomly choose n genes from the PPARα KO gene expression dataset and calculated the ES value. This process was repeated for 10^5 times and the frequency distribution of the resultant 10^5 ES values, which resembles normal distribution, was plotted. The mean (μ) and standard deviation (δ) of this distribution and z-score of the ES_0 value $((ES_0-\mu)/\delta)$ were calculated,. A statistically significant ES_0 should be significantly smaller than μ and has a negative z-score. The z-score was then converted to a p-value. The same procedure was applied on the set of genes up-regulated in NELF-B KO mice. In this case, the ES_0 value was expected to be larger than μ, and thus have a positive z-score. A similar comparison was made between NELF-B KO and ERRα KO (Figure S3C) (Dufour et al., 2007).

SUPPLEMENTAL FIGURE LEGENDS

Figure S1. Loss of NELF-B results in cardiomyopathy, related to Figure 1. **(A)** A scheme for animal breeding, inducible deletion, and analysis. **(B)** A representative genotyping result for the whole-body deletion of NELF-B. **(C)** H&E staining of heart tissue of various genotypes. Scale bar = 100 μm. **(D)** Neutrophil staining and quantification. n = 3. * $p < 0.05$. (**E**) Immunohistochemistry of NELF-B in control and NELF-B KO myocardium. Scale bar = 10 μm. Unless otherwise indicated, n = 4 mice per group were used in this and the following experiments.

Figure S2. Cardiomyocyte-specific NELF-B deletion, related to Figure 1. **(A)** A representative genotyping result for the cardiomyocyte-specific deletion of NELF-B. Heart tissue was used for the genotyping. **(B)** RT-PCR analysis of NELF-B mRNA in control (Ctrl) and cardiomyocyte-specific NELF-B KO (KO) heart tissue. **(C)** H&E staining of heart tissue from Ctrl and cardiomyocyte-specific KO mice. Scale bar = 50 μm. **(D)** Picrosirius red staining for the extent of collagen deposition in Ctrl and cardiomyocyte-specific KO heart tissue. Scale bar = 50 μm. **(E)** Relative mRNA levels of two hypertrophy markers. * $p < 0.05$. Error bars represent standard error of the mean (s.e.m.).

Figure S3. Gene expression analysis of NELF-B KO myocardium, related to Figures 2 and 3. **(A)** RT-PCR results showing the reduction of metabolism-related genes in the cardiomyocyte-specific KO myocardium. **(B)** Immunoblots for Cpt1b and Idh3g in

control and whole-body KO heart tissue. A Ponceau S-stained membrane was used as the loading control. Densitometric quantitation is shown on the right. * $p < 0.05$. ** $p < 0.001$. Error bars represent standard error of the mean (s.e.m.). **(C)** Graphs indicating overlap in down- and up-regulated genes in NELF-B and ERRα KO hearts as quantified by gene set enrichment analysis. The green and red squares denote the ES_0 values of down- and up-regulated genes, respectively. **(D)** Immunoblots of PPARα, RXRα, and PCG-1α in Ctrl and NELF-B KO myocardium. (**E**) Immunoblots of Cdk9 and cyclin T1 in Ctrl and KO myocardium. Ponceau S staining of total lysates was used as the loading control.

Figure S4. NELF influences chromatin binding of transcription initiation factors. **(A)** ChIP of NELF-A in Ctrl and NELF-B KO samples. (**B**) ChIP of phospho-serine 5 Pol II. (**C**) NELF-A and NELF-C/D ChIP at the TSS of Lpl and Myl3, two genes whose mRNA levels were not affected by NELF-B KO based on gene expression profiling. (**D**) Ratios of Pol II ChIP signals at TSS over gene body of Lpl and Myl3. (**E**) TFIID (TBP) ChIP at TSS of the metabolic genes. (**F**) ChIP of TFIIB and TFIID (TBP) at TSS of the metabolism-unrelated genes. (**G**) ChIP of histone H3 at various regions of the Ech1 gene shows low nucleosomal density at TSS. All results are average of ChIP experiments using three pairs of control and KO animals. * $p < 0.05$.

REFERENCES FOR SUPPLEMENTAL INFORMATION

Aiyar, S.E., Sun, J.-L., Blair, A.L., Moskaluk, C.A., Lv, Y., Ye, Q.-N., Yamaguchi, Y., Mukherjee, A., Ren, D.-M., Handa, H., *et al*. (2004). Attenuation of estrogen receptor alpha-mediated transcription through estrogen-stimulated recruitment of a negative elongation factor. Genes & Dev *18*, 2134-2146.

Amleh, A., Nair, S.J., Sun, J., Sutherland, A.E., Hasty, P., and Li, R. (2009). Mouse Cofactor of BRCA1 (Cobra1) is Required for Early Embryogenesis. PloS One *4*, e5034.

Chiao, Y.A., Ramirez, T.A., Zamilpa, R., Okoronkwo, S.M., Dai, Q., Zhang, J., Jin, Y.F., and Lindsey, M.L. (2012). Matrix metalloproteinase-9 deletion attenuates myocardial fibrosis and diastolic dysfunction in ageing mice. Cardiovasc Res *96*, 444-455.

Dufour, C.R., Wilson, B.J., Huss, J.M., Kelly, D.P., Alaynick, W.A., Downes, M., Evans, R.M., Blanchette, M., and Giguere, V. (2007). Genome-wide orchestration of cardiac functions by the orphan nuclear receptors ERRalpha and gamma. Cell Metab *5*, 345-356.

Gao, X., Zhang, Q., Meng, D., Isaac, G., Zhao, R., Fillmore, T.L., Chu, R.K., Zhou, J., Tang, K., Hu, Z., *et al*. (2012). A reversed-phase capillary ultra-performance liquid chromatography-mass spectrometry (UPLC-MS) method for comprehensive top-down/bottom-up lipid profiling. Anal Bioanal Chem *402*, 2923-2933.

Kuhn, K., Baker, S.C., Chudin, E., Lieu, M.H., Oeser, S., Bennett, H., Rigault, P., Barker, D., McDaniel, T.K., and Chee, M.S. (2004). A novel, high-performance random array platform for quantitative gene expression profiling. Genome Res *14*, 2347-2356.

Lin, J., Lopez, E.F., Jin, Y., Van Remmen, H., Bauch, T., Han, H.C., and Lindsey, M.L. (2008). Age-related cardiac muscle sarcopenia: Combining experimental and mathematical modeling to identify mechanisms. Exp Gerontol *43*, 296-306.

Lindsey, M.L., Yoshioka, J., MacGillivray, C., Muangman, S., Gannon, J., Verghese, A., Aikawa, M., Libby, P., Krane, S.M., and Lee, R.T. (2003). Effect of a cleavage-resistant collagen mutation on left ventricular remodeling. Circ Res *93*, 238-245.

Sun, J., Pan, H., Lei, C., Yuan, B., Nair, S.J., April, C., Parameswaran, B., Klotzle, B., Fan, J.B., Ruan, J., *et al*. (2011). Genetic and genomic analyses of RNA polymerase II-pausing factor in regulation of mammalian transcription and cell growth. J Biol Chem *286*, 36248-36257.

Sun, J., Watkins, G., Blair, A.L., Moskaluk, C., Ghosh, S., Jiang, W.G., and Li, R. (2007). Deregulation of cofactor of BRCA1 expression in breast cancer cells. J Cell Biochem *107*, 131-139.

Figure S1. Loss of NELF-B results in cardiomyopathy
Related to Figure 1

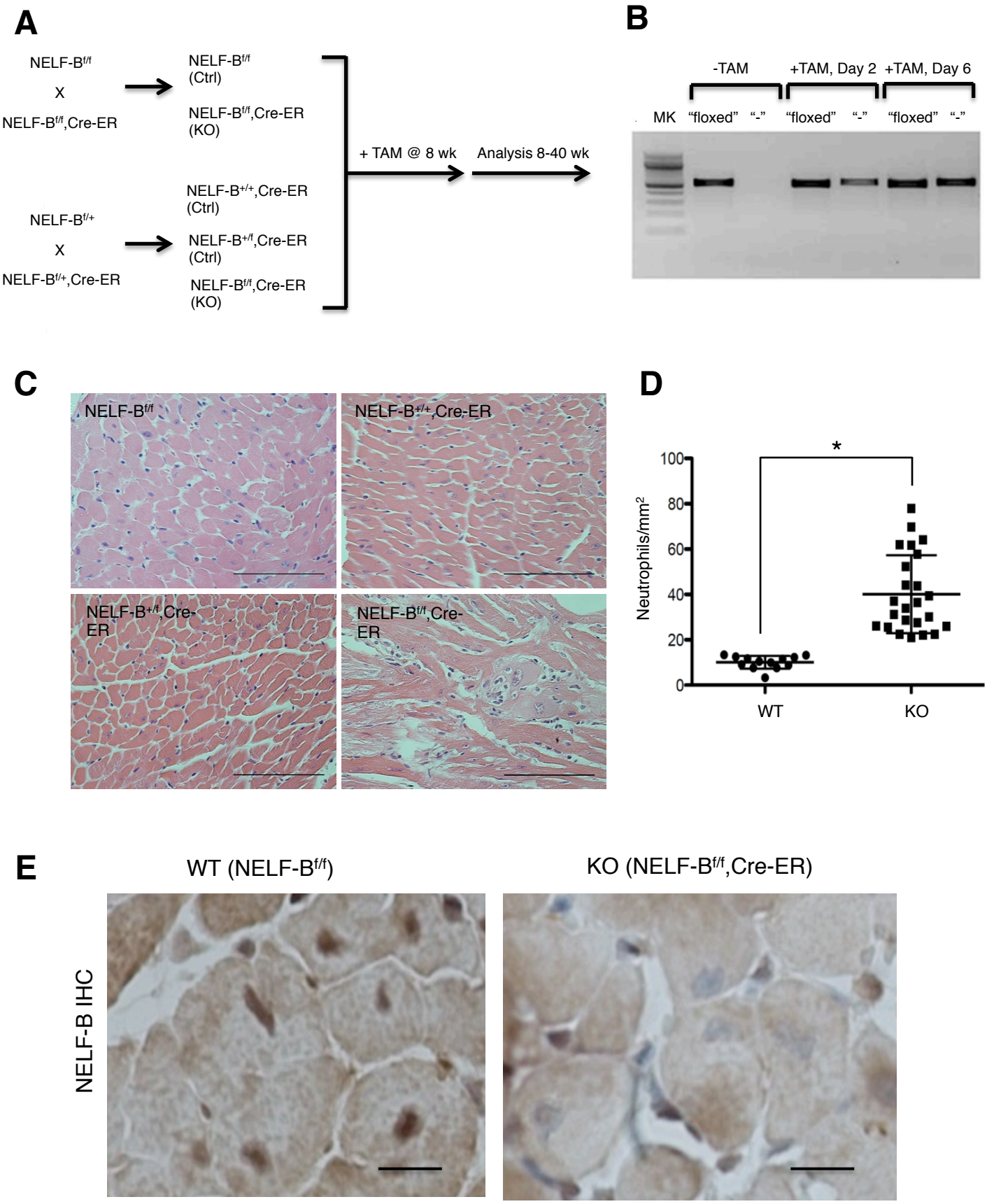

Figure S2. Cardiomyocyte-specific NELF-B deletion
Related to Figure 1

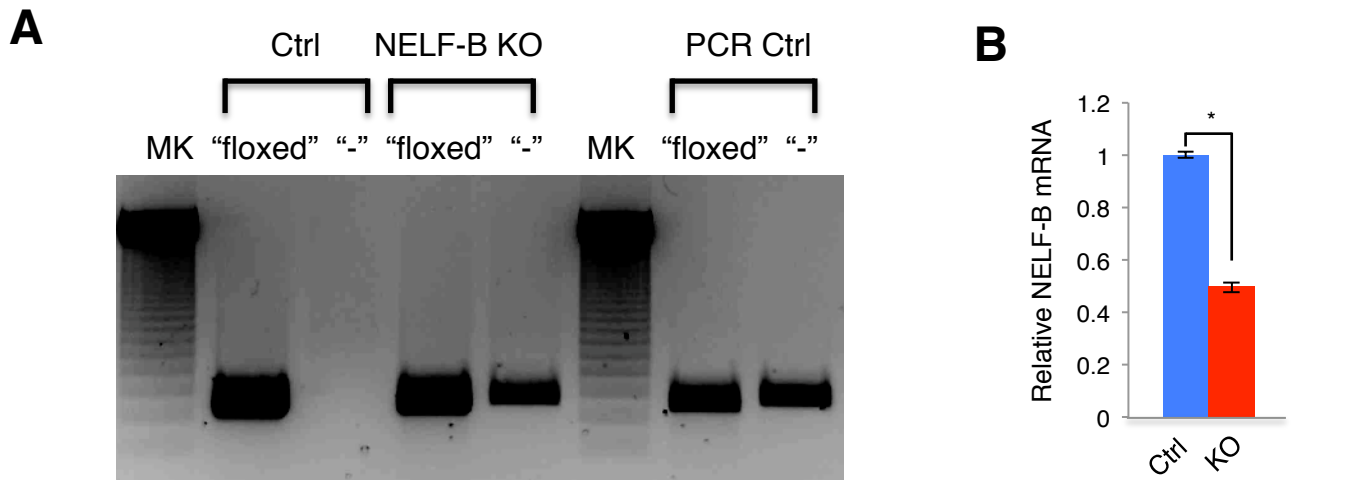

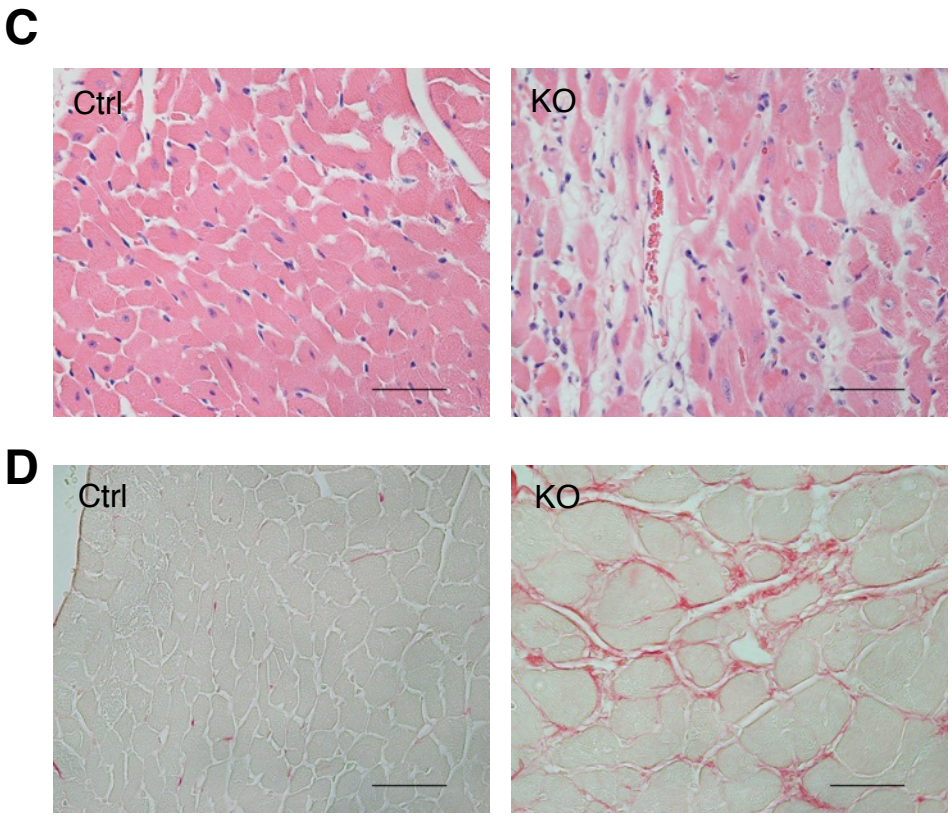

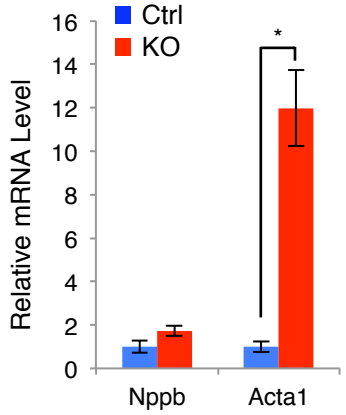

Figure S3. Gene expression analysis of NELF-B KO myocardium
Related to Figures 2 and 3

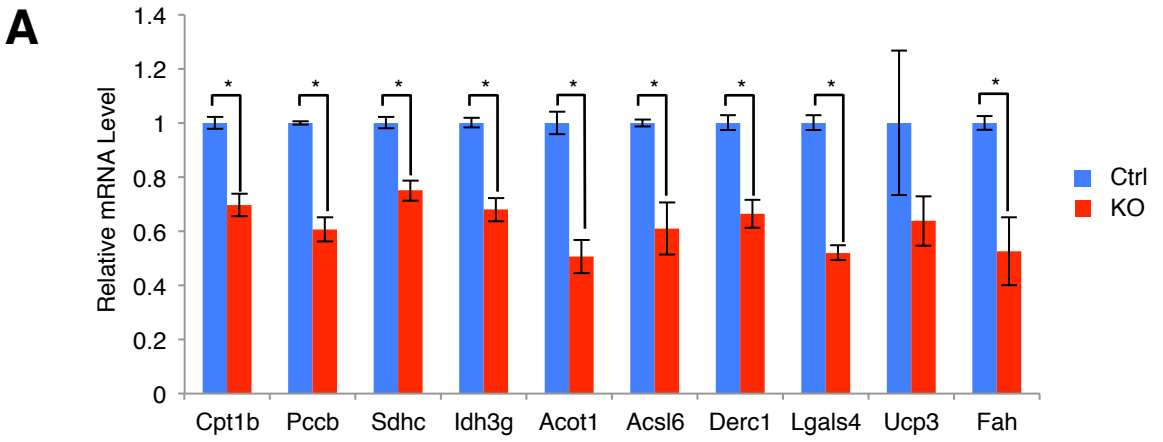

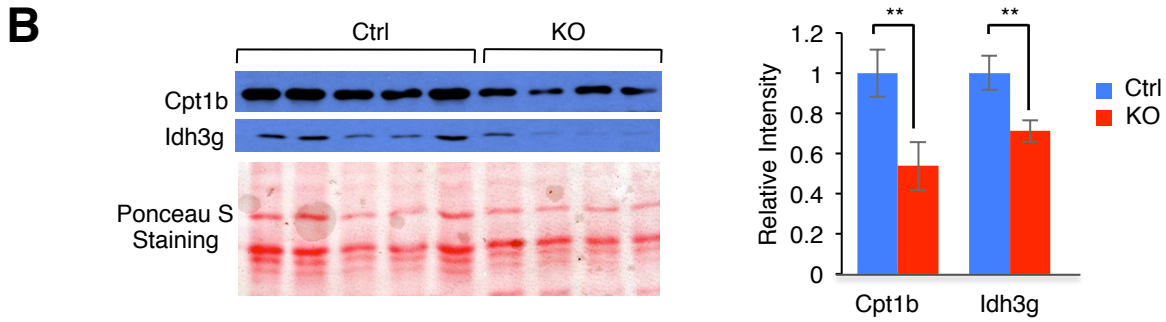

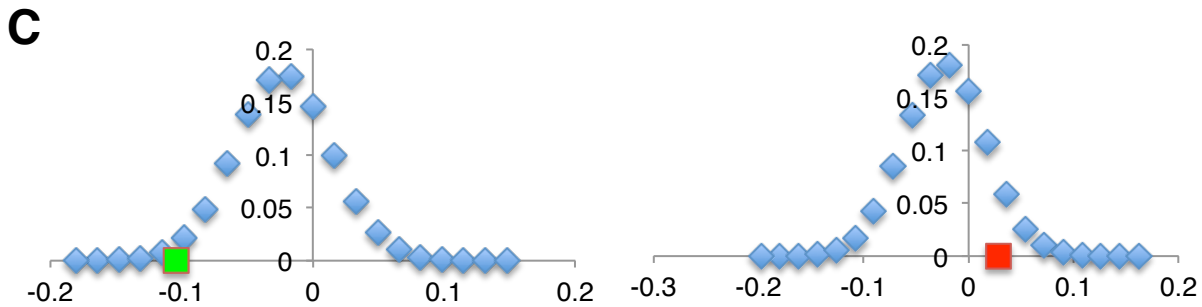

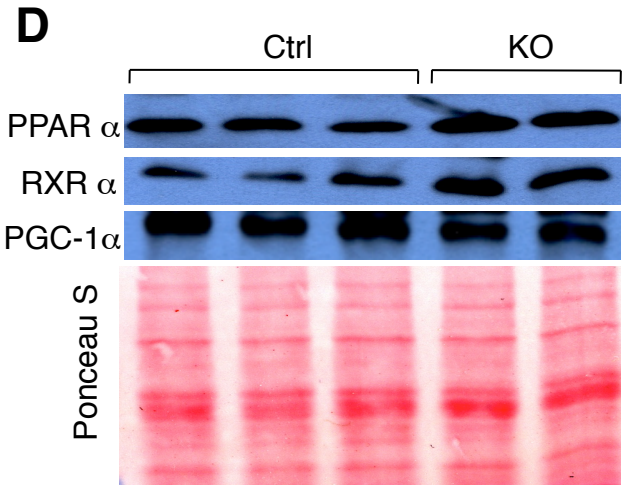

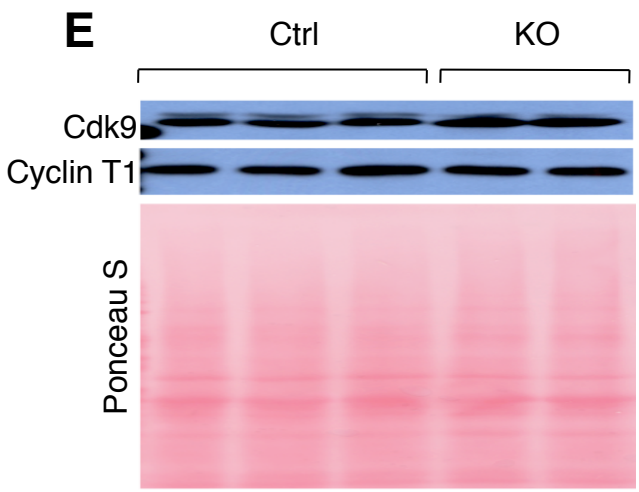

Figure S4. NELF influences chromatin binding of transcription initiation factors. Related to Figure 4

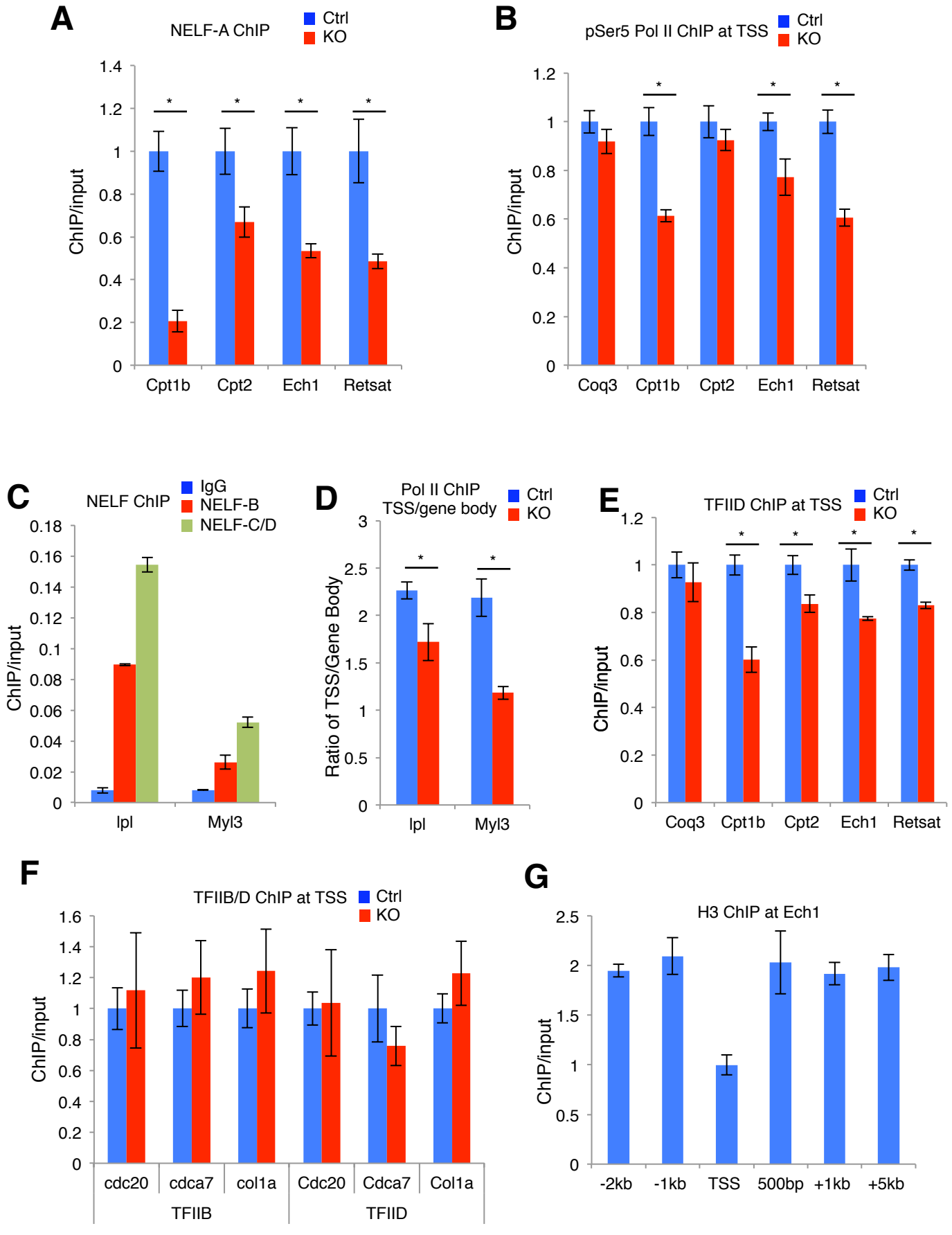

Supplementary Table S1. Echocardiography data for WT and KO mice at weeks 8, 16, 24, and 32 under baseline and dobutamine-stressed conditions.

		WT				KO			
		W8	W16	W24	W32	W8	W16	W24	W32
HR (bpm)	Baseline	457±14	425±7	422±9	408±13	427±10	442±9	424±8	369±17
	Dobutamine	579±10*	528±5*	539±10*	516±13*	573±3*	519±10*	488±9*	416±35*
EDD (mm)	Baseline	3.71±0.07	3.47±0.09	3.69±0.13	3.84±0.07	3.60±0.08	3.62±0.09	3.71±0.1	3.59±0.08#
	Dobutamine	3.15±0.07*	3.05±0.09*	3.06±0.08*	3.07±0.12*	2.93±0.09*	3.06±0.07*	3.07±0.08*	2.97±0.13*
ESD (mm)	Baseline	2.43±0.08	2.16±0.13	2.54±0.18	2.81±0.09	2.39±0.12	2.41±0.1	2.60±0.15	2.68±0.15
	Dobutamine	1.48±0.06*	1.51±0.13*	1.48±0.16*	1.48±0.12*	1.30±0.07*	1.50±0.05*	1.59±0.17*	1.85±0.21*
FS (%)	Baseline	34±1	38±2	32±3	27±2	34±2	34±2	30±2	26±3
	Dobutamine	53±2*	51±3*	52±4*	52±3*	57±1*	51±1*	49±4*	39±5*#

HR, heart rate; EDD, end diastolic dimension; ESD, end systolic dimension; FS, fractional shortening. WT: n=11; KO; n=8. * $p < 0.05$ vs corresponding baseline values; # $p < 0.05$ vs 32 weeks old WT after dobutamine treatment.

symbol	fold_change
Atic	-1.37
Tnfaip8	-1.37
Ube4b	-1.32
EG625054	-1.36
Tesc	-1.66
Mrpl54	-1.33
Maob	-1.36
Slc40a1	-1.82
Lrp4	-1.32
Rps13	-1.32
Rps12	-1.34
Trip6	-1.345
Nope	-1.45
Hrc	-1.47
Fah	-1.71
Rangrf	-1.53
Tmod4	-1.66
Abhd11	-1.53
Cpt1b	-1.59
Fntb	-1.4
Rpl39	-1.57
Tceb3	-1.45
Rpl34	-1.31
D0H4S114	-1.46
Commd10	-1.39
Ech1	-1.52
Rgs6	-1.32
Emg1	-1.31
LOC1000395	-1.46
LOC1000441	-1.32
Bcas2	-1.38
Bcas3	-1.33
Coq3	-1.37
Il1rl1l	-1.39
Lamb2	-1.42
Gstt1	-1.4
Acads	-1.38
Cirbp	-1.36
Art1	-1.55
Sgcb	-1.675
Sgca	-1.45

Fkbp10	-1.32
Sepw1	-1.35
Pcbp2	-1.31
Mdh2	-1.45
Myadm	-1.37
Ephx2	-1.69
Setx	-1.31
Maged2	-1.35
LOC641240	-1.31
Rabac1	-1.405
Cpt2	-1.34
Aarsd1	-1.32
Ccdc12	-1.44
LOC1000395	-1.33
Ptpre	-1.865
Acta2	-1.535
Pdk4	-3.13
LOC1000479	-1.81
Ssbp1	-1.43
Abhd1	-1.35
Spr	-1.31
Mid1ip1	-1.47
Acot1	-2.35
LOC1000481	-1.41
1110001J03F	-1.87
Socs2	-1.34
Dhrs7	-1.325
Dhrs4	-1.56
Pkig	-1.425
Slc35b1	-1.51
Angptl4	-1.71
Impdh2	-1.43
Rpl12	-1.36
Art5	-1.88
Mlxipl	-1.39
Ndufb10	-1.69
Rpl19	-1.31
Lgals4	-2.535
Ppp1r1a	-1.39
Hsd17b10	-1.35
Pdha1	-1.31
Mrps28	-1.73

2600009E05I	-1.43
Pccb	-1.77
Rps16	-1.35
AI593442	-1.39
LOC1000477(	-1.42
Cidea	-1.4
S100a13	-1.52
Snapin	-1.34
Tmem82	-1.41
Ahsa1	-1.33
Mvp	-1.31
Phpt1	-1.43
Art3	-1.31
Calm2	-1.42
Calm3	-1.4
Idh3g	-1.495
Sepx1	-1.305
D030028O16	-1.46
Gstm4	-1.33
Gstm5	-1.54
Rpap1	-1.33
Hist1h2ao	-1.42
4933426M11	-1.41
Hist1h2ah	-1.31
Myl1	-1.78
Scn4b	-1.5
Phkg1	-1.89
Gusb	-1.36
Fam131a	-1.51
Mrpl27	-1.42
Hspb3	-1.37
Mrpl23	-1.42
Fxyd1	-1.335
Spag7	-1.61
Mif4gd	-1.52
Mgst3	-1.34
Tmem109	-1.33
Mgst1	-1.41
Rcsd1	-1.47
Med16	-1.47
Tmem100	-1.4
Txnrd2	-1.33

Ywhag	-1.64
Ensa	-1.44
BC026585	-1.58
Nenf	-1.35
Nfu1	-1.46
Sod1	-1.31
Dnajc27	-1.33
Cryab	-1.39
Acadvl	-1.37
Aldoa	-1.4
Rps25	-1.4
Rps3a	-1.54
Sdhc	-1.51
1110036O03	-1.39
Sdhd	-1.31
Cd74	-1.45
Rsn	-1.49
Gpt1	-1.4
Mrpl16	-1.5
Bri3	-1.36
Arpc1b	-1.33
Prdx5	-1.33
Trap1	-1.4
Gtf3c1	-1.46
Ier3	-1.86
Slc25a34	-1.385
Trpc4ap	-1.35
Slc25a39	-1.51
Ctdsp1	-1.305
Sfrs16	-1.4
Uqcrc1	-1.43
C030006K11	-1.33
Sdpr	-1.48
Vbp1	-1.31
Phax	-1.35
2900010M23	-1.67
Sorcs2	-1.32
Ppm1k	-1.45
Ebpl	-1.34
Eif3f	-1.43
4930402H24	-1.6
Npm3-ps1	-1.43

Ces3	-1.6
Sfrs14	-1.33
Eif4ebp1	-1.44
Tnni3	-1.95
Tmem86a	-1.42
Gstk1	-1.35
LOC1000484	-1.63
Rdm1	-1.72
2310076L09	-1.565
9130213B05	-1.355
Fkbp11	-1.47
Tmem50a	-1.37
Psme1	-1.475
LOC677317	-1.62
Fabp3	-1.31
Yeats4	-1.455
Ddrgk1	-1.41
Cs	-1.4
Cox7a1	-1.42
Dusp23	-1.52
Irx3	-1.9
Mod1	-1.4
Gm2a	-1.37
Pnck	-1.35
Galk1	-1.33
Psmb5	-1.33
Rps21	-1.36
Psmd14	-1.31
Ak1	-2.75
Hcn2	-1.89
Mif	-1.31
Eif3k	-1.54
Snf8	-1.36
Fbp2	-2.88
Rrbp1	-1.33
Actr3	-1.38
Lrg1	-1.61
Npm3	-1.365
Rpl36a	-1.75
Fhod1	-1.33
LOC1000472	-1.4
Lrrc8	-1.4

Retsat	-1.7
Aamp	-1.57
LOC333331	-1.31
Sord	-1.53
Ndufs3	-1.31
Gm1673	-1.43
Glrx	-1.47
Thoc3	-1.35
Trappc2l	-1.31
1500012F01I	-1.42
Rps10	-1.36
Lypd2	-1.46
1700025K23I	-1.5
Ndufb9	-1.38
2-Mar	-1.36
A730008L03I	-1.725
Ndufb5	-1.41
Rshl2a	-1.36
Etfdh	-1.38
Gaa	-1.4
Rps5	-1.43
LOC1000442(	-1.31
Rps2	-1.38
Robld3	-1.31
Myoz2	-1.31
Decr1	-1.41
Hfe	-1.48
Ddah2	-1.35
Rps8	-1.32
Aplnr	-1.53
Pygo2	-1.39
Gstp2	-2.04
Epb4.1l3	-1.365
Myh9	-1.45
Lsm10	-1.42
Fyco1	-1.43
Hr	-1.62
Igtp	-1.38
Zxda	-1.33
F730014I05R	-1.36
Atp6v0e2	-1.44
Kptn	-1.4

Acy3	-1.55
Klra19	-1.46

Table S3. Metabolites exhibiting significant differences in relative quantity in left ventricles of KO mice compared to WT

Metabolite	$\log_2$(KO/WT)[1]	*t*-Test[2]
Acyl-carnitines[3]		
6:0	-0.89	0.0436
16:0	-1.52	0.0109
18:0	-2.51	0.0003
18:1	-1.33	0.0125
Ceramides[4]		
C8-Dihydroceramide	2.33	0.0002
Cer(32:1)	0.97	0.0014
Cer(33:1)	1.23	0.0009
Cer(34:1)	0.35	0.0192
Cer(36:1)	0.54	0.0003
Cer(36:2)	1.60	<0.0001
Cer(37:1)	0.65	0.0002
Cer(38:1)	0.34	0.0007
Cer(38:2)	0.23	0.0055
Cer(40:1)	0.23	0.0402
Cer(42:1)	0.27	0.0139
TCA cycle and related metabolites[5]		
Aconitate	1.38	0.0026
Citrate	1.20	0.0023
Succinate	0.57	0.0200
Hydroxyglutarate	0.75	<0.0001

[1] Ratio of normalized extracted ion current peak areas
[2] P-values, two-tailed Student's t-test
[3] Number of carbons:number of double bonds
[4] Shown in parentheses are the total number of carbons:total number of double bonds
[5] α-Ketoglutarate, malate and pyruvate did not exhibit significant differences in relative peak area; fumarate and oxaloacetate were not detected.

	Forward	Reverse
Cpt1b-TSS	GAGAGGCCAGACCCATACACC	CCCCAACTCACAGCTCAGGT
Cpt1b-1kb	GGGACCTGGAAGGCACAAGT	CTTGGGAACTGTCCTGGCTC
Idh3g-TSS	CCATACCCCGGATTTCTCG	TTAAGCACCGTTCTCGCGAC
Idh3g-1kb	AGCATAGGAGGCAGCTGTGG	TGGCAACAACATTGCTAGGG
Retsat-TSS	AGGACGCGGTCTTCCGAG	AGCAGAGCAGTGATCCACATGT
Acot1-TSS	CCTCCTCTTCCAGTCCAGCTC	AGGGCTCAAGGTTCAGCGT
Ech1-TSS	TCGGGAGTAAGTCGCACAGC	TCATCGCGGTAGCCATTTCT
Ephx2-TSS	AGCCAGCCTCCCCACTCTAG	TGACACAGACACGAAGCTGGA
Abdh1-TSS	CGCAAGCGGAAGAGTCAAAG	GGTATTCCATTTCCCAGGCTC
Cpt2-TSS	GGAAGTGCCCCTGTGGG	CACCCGTAGAGACTTAACGTCCA
Etfdh-TSS	TGGCTTGTATGTGACCCGG	CGCCACAGAGGACACGAAG
Derc1-TSS	CTCTGGACAAAATTCTCCCTTGA	CCGCCTGCTCCTTGCA
Coq3-TSS	GGGACCGGAAAAGGAGTAGG	GCCTTCCACCTCTCCACATC
Ucp3-TSS	CGTCAGATCCTGCTGCTACCT	AGTGCAGGGCCACCCTAAG
Leprel4-TSS	CACGTAGTGGACTCGAGCGTC	GGCTGGAATGCCTCTCTAGGA
Plin5-TSS	GGGATACATAGGGCATGAGCC	ACCCTCAGCTGTCCACGG
Fah-TSS	GAATCTAAAGGCCCTCGGCT	ACGGGACTATGCTTAGGGCA
Slc25a20-TSS	TCATTAGGGAAAGAGCCCCG	TCTACTTCCGGCTGCCCTC
Abat1-TSS	AAGCAAGGGCTAGAGGCAGTG	AAGCTTCGCCGAGCCAC
Fbp2-TSS	TCGGACTTTGGCACAGTCAAG	GCAGCCTCACAGCCTACTCG
Lgals4-TSS	AATGGCAGAACTGGAACCCAG	CCAGTGCACACGCAGCTG
Coq3-PBS	GGTAGCCCACGACCTTTGC	GCCACAAGCTCATAGAACGCA
Ech1-PBS	TGGGCCAAAGGTTTAAGCAA	GCACTCCTTCGTGTCTCATGTG
Retsat-PBS	CACTCCTGTGAGCCCAGCAT	TTGCCATGAATCTCCTGCCT
Cpt2-PBS	GCTGAGTCAGATGGGCACTGA	ACCTGGGTAAGGCACAGGC